6956–6969 *Nucleic Acids Research, 2011, Vol. 39, No. 16* *Published online 27 May 2011*
doi:10.1093/nar/gkr263

Nucleosomes protect DNA from DNA methylation *in vivo* and *in vitro*

Max Felle, Helen Hoffmeister, Julia Rothammer, Andreas Fuchs, Josef H. Exler and Gernot Längst*

Institut für Biochemie III, Universität Regensburg, Universitätsstr. 31, 93053 Regensburg, Germany

Received October 19, 2010; Revised February 22, 2011; Accepted April 6, 2011

ABSTRACT

Positioned nucleosomes limit the access of proteins to DNA. However, the impact of nucleosomes on DNA methylation *in vitro* and *in vivo* is poorly understood. Here, we performed a detailed analysis of nucleosome binding and nucleosomal DNA methylation by the *de novo* methyltransferases. We show that compared to linker DNA, nucleosomal DNA is largely devoid of CpG methylation. ATP-dependent chromatin remodelling frees nucleosomal CpG dinucleotides and renders the remodelled nucleosome a 2-fold better substrate for Dnmt3a methyltransferase compared to free DNA. These results reflect the situation *in vivo*, as quantification of nucleosomal DNA methylation levels in HeLa cells shows a 2-fold decrease of nucleosomal DNA methylation levels compared to linker DNA. Our findings suggest that nucleosomal positions are stably maintained *in vivo* and nucleosomal occupancy is a major determinant of global DNA methylation patterns *in vivo*.

INTRODUCTION

In mammals, DNA methylation occurs at CpG sites that are to 60–80% modified in a cell-type specific pattern and is generally associated with repressed states of chromatin (1–4). DNA methylation is involved in epigenetic processes such as differentiation, proliferation, transcriptional regulation, genomic imprinting, X-chromosome inactivation, silencing of repetitive elements, maintenance of genomic stability and DNA repair (2,3). Although some functional overlap exists (5), the DNA methyltransferases can be generally divided into two classes: the 'maintenance' DNA methyltransferase Dnmt1 maintains methylation patterns on the newly synthesized daughter strands during replication and the *de novo* DNA methyltransferases Dnmt3a and Dnmt3b introduce novel methylation marks in the genome (6).

The fundamental unit of chromatin is the nucleosome, composed of 147 bp of DNA wrapped around an octamer of H2A, H2B, H3 and H4 core histone proteins. Nucleosomes impose a significant barrier for sequence-specific recognition, impeding the access of regulatory proteins to DNA (7). However, chromatin presents the natural substrate for DNA-dependent processes like control of gene expression, DNA replication, recombination and repair (8,9). Therefore active mechanisms like ATP-dependent chromatin remodelling exist to alter chromatin structure in order to regulate DNA accessibility (7). Chromatin remodelling complexes comprise a highly diverse group of ATPases belonging to the SNF2 superfamily that have the capability to slide, evict or destabilize nucleosomes (10,11). The ATPases are present in a large number of different multiprotein complexes with specialized functions regarding the organization of chromatin and the regulation of DNA-dependent processes (11,12).

Chromatin remodelling enzymes also impact cellular DNA methylation. Deletion of the remodelling ATPase *DDM1* in *Arabidopsis* or its murine homolog *Lsh* results in a global loss of DNA methylation (13,14). Lsh was shown to recruit *de novo* DNA methyltransferases (15) and to cooperate with Dnmt3b in PRC and HDAC-mediated gene silencing (16,17). Mutations in the *ATRX* gene, belonging to the Rad54 subfamily (Snf2 family) (10) result in the ATR-X syndrome that is characterized by both hypo- and hypermethylation of rDNA repeats (18). Furthermore, the hSnf2H containing complex NoRC (19) represses rDNA transcription by recruiting DNA methyltransferase and histone deacetylase (20). Direct interaction of Dnmt1 with hSnf2H increased the affinity of Dnmt1 towards nucleosomes (21) and the *de novo* DNA methyltransferases Dnmt3a and Dnmt3b were found in complexes with Brg1 (22) and hSnf2H, respectively (23). But still, the question remains whether genomic DNA is globally rendered accessible by the ATP converting

*To whom correspondence should be addressed. Tel:/Fax: +49 89 5996 435; Email: gernot.laengst@vkl.uni-regensburg.de

remodelling enzymes or whether chromatin dynamics is restricted and therefore chromatin structure determines DNA methylation patterns.

The enzymatic properties of the DNA methyltransferases have been extensively studied on free DNA as substrate (24–29). However, functional studies on DNA methylation in chromatin are very limited and the results are not consistent. Nucleosomal DNA methylation was either shown not to be affected by Dnmt1 and Dnmt3a irrespective of the DNA sequence (30), to be significantly reduced for Dnmt1, Dnmt3a and Dnmt3b (21,31,32), or to be inhibited for Dnmt3a (33).

To evaluate the effect of positioned nucleosomes on the DNA methylation efficiency *in vitro* and *in vivo*, we performed high-resolution mapping of *de novo* DNA methylation events in reconstituted chromatin systems and quantified nucleosomal DNA methylation *in vivo*.

MATERIALS AND METHODS

Plasmids

Human Dnmt3a was PCR-amplified from IRATp970A0473D (RZPD), cut with BamHI/EcoRI and cloned into pENTR3C (Invitrogen) following LR-recombination into pDEST10 (Invitrogen). Human Dnmt3b2 (kind gift from F. Lyko) was PCR-amplified, cut with BamHI/NheI and cloned into a modified pET11 bacterial expression vector (Novagen) carrying an N-terminal Flag-tag and a C-terminal 6× His-tag (pETM). Sequences were verified by sequencing. Snf2H K211R point mutant [kindly provided by R. Shiekahattar (34)] was cloned with a C-terminal Flag-tag in pFastbac1 (Invitrogen). The plasmids pPCRScript_slo1-gla75, pGA4 BN601-m1, pMA BN601mod rDH70_Cless were used for PCR amplification of DNA fragments for chromatin reconstitution.

Protein purification

Induction of Dnmt3b2 expression (pETM-Dnmt3b2 N-Flag, C-His) in BL21 *Escherichia coli* cells was carried out at an OD_{600} of 0.5–0.6 with 1.0 mM IPTG for 3 h at 24°C.

Baculovirus carrying N-His Dnmt3a (pDEST10-Dnmt3a) or C-Flag Snf2H K211R were prepared as described (Invitrogen, Bac-to-Bac). The baculovirus for C-Flag Snf2H expression was generously provided by R. Kingston (35). 2.0×10^8 Sf21 insect cells were infected for 48–60 h and cells stored at −80°C until use.

All purification steps were performed on ice. Protease inhibitors PMSF (1.0 mM), Leupeptin (1–10 μg/ml), Aprotinin, Pepstatin (1.0 μg/ml) were added to buffers prior to use.

Preparing cell lysates

Sf21 insect cells ($2.0–2.5 \times 10^8$) resuspended in 10 ml lysis buffer were lysed by three repeated freeze-thaw cycles and subsequently treated with five strokes each of A-type and B-type pestle in a dounce homogenizer. Cells were further treated by sonification with a Branson Sonifier 250D (3× for 30 s 50% amplitude, 50% duty cycle) following clearance by centrifugation (30 min, 20 000*g*, 4°C). *Escherichia coli* cells were resuspended in lysis buffer (10 ml/1.0 g cells) supplemented with lysozyme (1.0 mg/1.0 ml lysate) following incubation for 30 min at 4°C. Cells were treated with five strokes of a B-type dounce homogenizer and sonified following clearance by centrifugation.

Purification of C-Flag Snf2H

Sf21 cell lysate was prepared in EX-500 buffer (500 mM KCl, 20 mM Tris buffer pH 7.6, 10% glycerol, 1.5 mM $MgCl_2$, 0.5 mM EGTA) supplemented with 0.1% NP-40. The cleared lysate was incubated with 200 μl M2-affinity gel (Sigma) for 2 h at 4°C After washing (3× with lysis buffer) proteins were eluted with one bed volume of buffer EX-300 supplemented with 0.05% NP-40 and Flag peptide (400 ng/μl). Eluted proteins were directly snap frozen in liquid nitrogen and stored at −80°C.

Purification of Dnmt3a and Dnmt3b2

Prior to use all buffers were supplemented with 5 mM ß-mercaptoethanol. Dnmt3a/Dnmt3b2 cell lysates were prepared in lysis buffer (20 mM Tris, pH 7.5; 10% glycerol; 500 mM NaCl; 0.5% NP-40; 5.0 mM imidazole) and incubated with Ni-NTA agarose (Qiagen). 'Beads' were washed once with five bead volumes of lysis buffer and three times with wash buffer 1 (20 mM Tris pH 7.5; 10% glycerol; 500 mM NaCl, 40 mM imidazole, 0,1% NP-40). Dnmt3a was in addition washed twice with wash buffer 2 (20 mM Tris 7.5; 10% glycerol; 10 mM NaCl, 0.1% NP-40). Bound proteins were batch-eluted with the addition of elution buffer (D3a: 20 mM Tris, pH 7.5; 10% glycerol; 10 mM NaCl; 1000 mM imidazole, 2.0 mM EDTA, 0.1% NP-40; D3b2: 20 mM Tris, pH 7.5; 10% glycerol; 250 mM NaCl; 250 mM imidazole, 2.0 mM EDTA, 0.1% NP-40). Elution fractions were combined, dialyzed against buffer SP-200 (200 mM NaCl, 20 mM Tris, 7.5, 2.0 mM $MgCl_2$, 1.0 mM EDTA, 10% glycerol, 0.05% NP-40) and loaded onto a SP FF column (GE Healthcare). Dnmt3a and Dnmt3b2 were step-eluted with SP-400 and SP-500 buffer, respectively. Peak fractions were combined, dialyzed against SP-200 buffer and snap frozen in small aliquots in liquid nitrogen and stored at −80°C.

Nucleosome reconstitution by salt gradient dialysis

Chromatin assembly of DNA fragments with histone octamers from *drosophila* using the salt dialysis technique was performed as previously described (36) A typical assembly reaction (50 μl) contained 5.0 μg DNA, varying amounts of histone octamer, 200 ng BSA/μl, and 250 ng competitor DNA in high salt buffer (10 mM Tris, pH 7.6, 2.0 M NaCl, 1.0 mM EDTA, 0.05% NP-40, 2.0 mM ß-mercaptoethanol). The salt was continuously reduced to 200 mM NaCl during 16–20 h. The quality of the

assembly reaction was analysed on a 5.0% PAA in 0.4× TBE following ethidium bromide staining.

Nucleosome mobility assay

Nucleosome remodelling reactions were performed as described (12). Briefly, reaction mixes in RB90 buffer (20 mM Tris, pH 7.6, 1.5 mM $MgCl_2$, 1.0 mM EDTA, 10% glycerol, 90 mM KCl, 1.0 mM DTT) supplemented with 1.0 mM ATP and 200 ng BSA/μl containing 200 ng (1.0 picomol) reconstituted L78-NPS2-L79 and 50–200 ng (0.5–2.0 picomol) Snf2H were incubated for 90 min at 26°C. Remodelling reactions were stopped by the addition of 50–100 ng competitor DNA (pCpGL-basic, 0.25–0.5 femtomol) and nucleosome positions were analysed by native PAGE. The non-hydrolysable ATPγS and the mutant Snf2H K211R were used as substitutes for ATP and WT Snf2H, respectively.

Electromobility shift assay

Electromobility shift assays (EMSAs) with Dnmt3a and Dnmt3b2 were performed in 20 μl reaction volume in 20 mM Tris, pH 7.6, 30 mM KCl, 5.0 mM EDTA, 1.0 mM DTT, 5.0 μM SAM, 20% glycerol. Reconstituted nucleosomes were incubated with Dnmt3a/b2 for 15 min at 26°C to allow for complex formation. Reactions were put on ice, loaded onto a 5.0% PAA gel in 0.4× TBE and the DNA was visualized by ethidium bromide staining.

Isolation of endogenous nucleosomal DNA by MNase digest

Digestion of chromatin from Hela cells (2×10^7) was performed with micrococcal nuclease (MNase Sigma; 100–1000 U) in 3.0 ml permeabilization buffer (15 mM Tris, pH 7.6, 300 mM sucrose, 60 mM KCl, 15 mM NaCl, 4.0 mM $CaCl_2$, 0.5 mM EGTA, 0.2% NP-40, 0.5 mM ß-mercaptoethanol) for 3 min at 37°C. The nuclease reaction was stopped by addition of 3.0 ml stop buffer (50 mM Tris, pH 8.0, 20 mM EDTA, 1.0% SDS). RNA was degraded with 250 μg RNAse A for 2 h at 37°C and cellular proteins digested with 250 μg proteinase K at 37°C overnight. Nucleosomal DNA recovered after ethanol precipitation was subjected to separation on 1.5% agarose gels in 1× TBE. Clearly separated 1 n, 2 n, 3 n nucleosomal DNAs were excised from the gel and DNA was eluted using the BioRAD Electro-Eluter according to the manufacturer's protocol. Purity of nucleosomal DNA preparations was analysed by agarose gel electrophoresis.

Micellar capillary electrophoresis

Sample preparation of mononucleosomal and HeLa genomic DNA was adapted from the protocol established by Fraga (37). Briefly, DNA Samples (10 μl, ~2 μg/μl) were heated for 5 min at 95°C and cooled on ice. After addition of 4 μl Milli-Q grade H_2O, 1 μl 10 mM $ZnSO_4$ and 2 μl P1 nuclease (Sigma-Aldrich, reconstituted to 250 U/ml in 30 mM sodium acetate), samples were digested over night at 37°C. Dephosporylation was performed by the addition of 2 μl of 500 U/ml antarctic phosphatase (NEB, in 50 mM Tris–HCl pH 7.6, 5 mM $MgCl_2$) for 2 h at 37°C. For CE analysis samples were concentrated by lyophilization and redissolving the samples in 4–10 μl Milli-Q grade H_2O.

Micellar capillary electrophoresis of nucleosides was adapted from Fraga (37) to our PA800 ProteomeLab capillary electrophoresis system (Beckman-Coulter). Samples were injected by negative pressure 1.38 kPa (0.2 psi) for 10 s into an uncoated fused-silica capillary (100 μm ID, 67 cm total length, 57 cm effective length, Beckman Coulter) in running buffer (48 mM $NaHCO_3$, pH 9.6; 60 mM SDS). Separation was performed at 17 kV (electrical field strength 254 V/cm) for 13 min and UV absorption was monitored at 254 nm. Before and in between runs the capillary was rinsed with 1.0 M NaOH for 1 min, 1.0 mM NaOH for 2 min and running buffer for 3 min. Prior to the experiments the capillary was rinsed as described above and equilibrated at 17 kV for 1.0 h. We found that this significantly increased reproducibility. For reference, nucleosides 2′-deoxyadenosine (A), 2′-deoxythymidine (T), 2′-deoxyguanosine (G), 2′-deoxycytidine (C) (Sigma-Aldrich) and 5-methyl 2′-deoxycytidine (5-meC; Biomol GmbH) were dissolved at 5.0 mM in Milli-Q grade H_2O.

We calculated the 5-meC content as percentage of the area 5-meC/area C + area 5-meC and found a 5-meC level for HeLa genomic DNA of 3.06% (±0.17%) (Figure 4D) consistent with previous findings (37). The 5-meC content of linker DNA was calculated as the difference of the 5-meC content (HeLa gDNA) and the 5-meC content (1 n). The relative 5-meC content of linker and nucleosomal DNA was determined considering an average nucleosomal repeat length of 188 bp in HeLa cells (38) and a nucleosome length of 147 bp. The total of methylated CpG sites was calculated as the percentage of the proportion of linker DNA added to the proportion of nucleosomal DNA multiplied with the relative nucleosomal 5-meC content.

In vitro DNA methyltransferase assay for Dnmt3a and Dnmt3b2

Typical *de novo* DNA methyltransferase reaction (50 μl) contained 100 nM Dnmt3a and Dnmt3b2, DNA template and oligonucleotides at 500 and 5000 nM CpG sites, respectively, 200 ng BSA/μl and 480 nM ^{3}H-SAM (GE Healthcare, TRK581-250UCi, 9.25 MBq with 1.0 mCi/ml and 63.0 Ci/mmol) in DNA methyltransferase buffer (20 mM Tris, pH 7.6, 1.0 mM EDTA, 1.0 mM DTT). The reaction was started with the addition of DNA, incubated at 37°C for 10–30 min, and stopped with 10 μl of 10 mM SAM (Sigma). The reaction was spotted on DE81 filter (Whatman), washed three times with 0.2 M NH_3HCO_3, once with water and ethanol following drying and scintillation counting.

DNA methylation mixtures (25 μl) added to nucleosome mobility reactions (25 μl), contained 200 nM Dnmt3a/b2,

200 ng BSA/μl, 960 nM ^{3}H-SAM in 40 mM Tris, pH 7.6, 4.0 mM EDTA, 2.0 mM DTT.

Bisulfite conversion and analysis of CpG site methylation

Site-specific DNA methylation analysis was performed with the C91-NPS2-C104 DNA fragment (342 bp, 27 CpG sites) as free DNA or fully reconstituted mononucleosome. DNA methylation reactions (40 μl) with 600 nM Dnmt3a or 200 nM Dnmt3b2 were carried out in DNA methyltransferase buffer (20 mM Tris, pH 7.6, 1.0 mM EDTA, 1.0 mM DTT) with 200 ng BSA/μl, 250 μM SAM (SIGMA) and template at 1800 and 20 nM CpG sites, respectively. Reactions with M.SssI contained 4 U of enzyme and 20 nM CpG sites in 1× NEB buffer 2. The reactions were incubated for 4 h at 37°C following heat-inactivation at 65°C for 20 min. DNA methylation reactions were processed according to the Epitect bisulfite conversion kit (Qiagen). The upper (+) and the lower strand (−) of the bisulfite-converted DNA were PCR-amplified with primer pairs MF81/82 and MF112/113.

PCR fragments were cloned into the pGEM-T-EASY vector (Promega) according to the manufacturer's instructions, and the DNA from positive clones was sent for sequencing. Analysis and quality control of bisulfite-converted DNA was done with BiQ ANALYZER software (http://biq-analyzer.bioinf.mpi-inf.mpg.de/) provided by C. Bock (39). The DNA methylation frequency of each CpG site was plotted against the respective CpG dinucleotides of the DNA sequence.

D3A DNA (+) 32 clones, D3A DNA (−) 39 clones, D3A nuc (+) 29 clones, D3A nuc (−) 44 clones, D3b2 DNA (+) 31clones, D3b2 DNA (−) 37 clones, D3b2 nuc (+) 25 clones, D3b2nuc (−) 22 clones, M.SssI DNA (+) 22 clones, M.SssI DNA (−) 23 clones, M.SssI nuc (+) 19 clones, M.SssI nuc (−) 21 clones.

DNA fragments

DNA fragments containing a modified nucleosome positioning sequence 601 (40) (referred to as NPS1, 147 bp, 3 CpG sites) are flanked by a partial rDNA promoter sequence (~80 bp) on the left and a partial HSP70 promoter sequence (~85 bp) on the right. By using different combinations of oligonucleotides, symmetrical and asymmetrical linker DNA of variable length, relative to the NPS sequence, can be generated.

In addition, two other DNA fragments were designed for DNA methylation studies. Both carry a CpG site supplemented modified 601 nucleosome positioning sequence (15 CpG sites, referred to NPS2), but differ in their CpG content of their flanking DNA overhangs. For DNA methylation studies, either new CpG sites were introduced into the linker DNA (referred to as 'C' precedent to the number for the linker length) or completely mutated (referred to as non-CpG 'N').

The DNA fragments were amplified by PCR and purified DNA fragments were subsequently used for nucleosome assembly reactions. Due to oligonucleotide annealing the NPS1 used consists of 142 bp instead of 147 bp.

Template	Primer (forward)	Primer (reverse)	DNA template	length
NPS1	AP7	AP8	pPCRScript_slo1-gla75	142
22-NPS1	AP3	AP8	pPCRScript_slo1-gla75	164
22-NPS1-22	AP3	AP13	pPCRScript_slo1-gla75	191
40-NPS1	AP5	AP8	pPCRScript_slo1-gla75	182
40-NPS1-40	AP5	AP14	pPCRScript_slo1-gla75	227
77-NPS1	AP1	AP8	pPCRScript_slo1-gla75	219
77-NPS1-77	AP1	AP15	pPCRScript_slo1-gla75	301
NPS2	MF124	MF125	pGA4 BN601-m1	150
C91-NPS2-C104	MF79	MF80	pGA4 BN601-m1	342
N78-NPS2-N79	MF133	MF134	pMA BN601mod rDH70_Cless	304

DNA sequences

NPS2 (150 bp, 15 CpG sites)
GATCCCGAATCCCGGTGCCGAGGCCGCTCAATT
GGTCGTAGCAACGTCTAGCACCGCTTAAACGCA
CGTACGCGCTGTCCCCCGCGTTTTAACCGCCAA
GGGGATTACTCCCTAGTCTCCAGGCACGTGTCA
GATATATACAGCTAG

C91-NPS2-C104 (342 bp, 27 CpG sites)
GAATTGGGTACCAGATCTTTTGAGGTCCGGTTC
TTTTCGTTATGGGGTCATATGTTTCGGCCACCTC
CCCATGGTACGACTTCCAGGTACGGATCCCGAA
TCCCGGTGCCGAGGCCGCTCAATTGGTCGTAGC
AACGTCTAGCACCGCTTAAACGCACGTACGCGC
TGTCCCCCGCGTTTTAACCGCCAAGGGGATTAC
TCCCTAGTCTCCAGGCACGTGTCAGATATATAC
AGCTAGCGACAAAGAAAACTCGAGAAATTTCTC
GTAAGGCCGTTATTCTCTAGATTCGTTTTGTGA
CGCTCCCTCTCCGTACTAAGATCTGAGCTCCAG
CTTTTGTTCCC

N78-NPS2-N89 (304 bp, 15 CpG sites)
TCTTTTGAGGTTGGGTTCTTTTGCTTATGGGGT
CATATGTTTGGGCCACCTCCCCATGGTATGACT
TCCAGGTATGGATCCCGAATCCCGGTGCCGAG
GCCGCTCAATTGGTCGTAGCAACGTCTAGCACC
GCTTAAACGCACGTACGCGCTGTCCCCCGCGTT
TTAACCGCCAAGGGGATTACTCCCTAGTCTCCA
GGCACGTGTCAGATATATACAGCTAGCTATGAA
AGAAAACTGCAGAAATTTCTCTTAAGGCAGTTA
TTCTCTAGATTGCTTTTGTGACTCTCCCTCTCTG
TACTAAG

NPS1 (142 bp, 3 CpG sites)
GATCCAGAATCCTGGTGCTGAGGCTGCTCAATT
GGTTGTAGCAAGCTCTAGCACTGCTTAAATGCA
TGTACGCGCGGTCCCCTGTGTTTTAACTGCCAA
GGGGATTACTCCCTAGTCTCCAGGCATGTGTCA
GATATATACA

77-NPS1-77 (301 bp, 9 CpG sites)
ATCTTTTGAGGTCCGGTTCTTTTCGTTATGGGG
TCATATGTTTGGGCCACCTCCCCATGGTATGAC
TTCCAGGTATGGATCCAGAATCCTGGTGCTGAG
GCTGCTCAATTGGTTGTAGCAAGCTCTAGCACT

GCTTAAATGCATGTACGCGCGGTCCCCTGTGTT
TTAACTGCCAAGGGGATTACTCCCTAGTCTCCA
GGCATGTGTCAGATATATACAGCTAGCTAGCAA
AGAAAACTCGAGAAATTTCTCTTAAGGCCGTTA
TTCTCTAGATTCGTTTTGTGACTCTCCCTCTCTG
TAC

Oligonucleotides

Name	Sequence 5′–3′
AP1	ATCTTTTGAGGTCCGGTTCTTT
AP3	CATGGTATGACTTCCAGGTATGG
AP5	ATGTTTGGGCCACCTCCCC
AP7	GATCCAGAATCCTGGTGCTGAG
AP8	TGTATATATCTGACACATGCCTGGA
AP13	TTTCTCGAGTTTTCTTTGCTAGCT
AP14	TAACGGCCTTAAGAGAAATTTCT
AP15	GTACAGAGAGGGAGAGTCACAAAAC
MF79	GAATTGGGTACCAGATCTTTTGAG
MF80	GGGAACAAAAGCTGGAGCTC
MF81	GAATTGGGTATTAGATTTTTTGAGGTT
MF82	AAAAACAAAAACTAAAACTCAAATCTTAATA
MF112	GGGAATAAAAGTTGGAGTTTAGATTTTA
MF113	AAATTAAATACCAAATCTTTTAAAATCC
MF124	GATCCCGAATCCCGGTG
MF125	CTAGCTGTATATATCTGACACGTGCC
MF133	TCTTTTGAGGTTGGGTTCTTTTG
MF134	CTTAGTACAGAGAGGGAGAGTCACAA

RESULTS

Dnmt3a and Dnmt3b2 have distinct nucleosome binding properties

In order to characterize the nucleosomal binding mode of the *de novo* methyltransferases, human Dnmt3a and Dnmt3b2 proteins were purified via their 6× His-tag from Sf21 and *E. coli* cells, respectively (Figure 1A). Importantly, a second purification step was included, involving a cation exchange matrix (SP FF, GE Healthcare), to remove associated DNA still present after affinity purification (Figure 1B, lanes 1–4). This is a critical purification step, avoiding unspecific methylation of the co-purified DNA, a potential problem in the interpretation of the results of previous studies (21,30).

Defined nucleosomal substrates with a single positioned nucleosome were reconstituted on DNA fragments containing a strong nucleosome positioning sequence at varying positions on the DNA (Figure 1C). We used a variant of the 601 nucleosome positioning sequence (40) (referred to as NPS1) that was extended at only one side (asymmetric nucleosomes containing only one linker) or at both sides (symmetric nucleosomes with two DNA linkers) with DNA linkers of varying length. DNA fragments were generated by PCR and reconstituted into nucleosomes by the salt dialysis method. Binding studies with increasing concentrations of Dnmt3a and Dnmt3b2 were performed using a mixture of free DNA and nucleosomes in competitive EMSAs (Figure 1D and Supplementary Figure S2).

Using the nucleosomal substrates 77-NPS1-77, 77-NPS1, NPS1 and the corresponding free DNA, Dnmt3a preferentially bound the symmetric 77-NPS1-77 nucleosome whereas the other substrates were bound with lower affinity (Figure 1D, lanes 1–4). Dnmt3a did preferentially bind to symmetric nucleosomes with longer linker DNA over symmetric and asymmetric nucleosomes with shorter linker DNA and free DNA (Supplementary Figure S2A and B, lanes 1–4). This pattern of binding suggests that Dnmt3a recognizes nucleosomal structures in addition to free DNA, resulting in a higher affinity towards nucleosomal DNA than to free DNA.

In contrast, Dnmt3b2 bound with similar affinity to free DNA and the 77-NPS1-77 nucleosome and with decreasing affinity to the 77-NPS1 nucleosome and the asymmetric and symmetric nucleosomes with even shorter DNA linkers (Figure 1D, lanes 5–8 and Supplementary Figure S2A and B, lanes 5–8). The data suggest a different binding mode for Dnmt3b2 compared to Dnmt3a in that Dnmt3b2 mainly recognizes free DNA and does not specifically recognize nucleosomal structures.

De novo methylation of nucleosomal DNA is strongly inhibited

To evaluate the extent of *de novo* DNA methylation of nucleosomes, three different templates with a modified 601 sequence (NPS2) containing additional CpG sites were reconstituted into chromatin. CpG sites were placed such that potential methylation sites were spread along the whole nucleosome positioning sequence. Nucleosomes were reconstituted either on DNA fragments containing DNA linkers with CpG sites or lacking DNA methylation sites. In contrast to the EMSAs, histone:DNA ratios were titrated such that DNA was completely reconstituted into mononucleosomes (Figure 2A). Nucleosomes were almost exclusively positioned on the NPS2 sequence as visualized by the discrete mononucleosomal band on the native polyacrylamide gel and as verified by a restriction enzyme accessibility assay (Supplementary Figure S3A and B).

De novo DNA methylation reactions were performed with each template either as free DNA or reconstituted into mononucleosomes (Figure 2, Supplementary Figure S4). The bacterial CpG-specific DNA methyltransferase M.SssI served as control for free DNA contaminations and to detect accessible CpG sites as it was shown not to methylate within nucleosomes (30,31,41). In addition we used M.SssI to normalize our methylation reactions and to reveal functional differences between the *de novo* methyltransferases.

Dnmt3a and Dnmt3b2-dependent DNA methylation efficiency of the C91-NPS2-C104 fragment (containing CpGs in the linker), was similar on free and nucleosomal DNA (Figure 2B), yielding a DNA:NUC methylation ratio of ~1.3 (Figure 2C, Supplementary Figure S4). Since the DNA methylation reactions are not endpoint reactions (Supplementary Figure S4), efficient methylation of the linker DNA is observed and similar methylation efficiencies were expected for the free DNA and nucleosomal DNA. In contrast, methylation of the linker-less NPS2 nucleosome was repressed by a factor of 36 and 27 for Dnmt3a and Dnmt3b2, respectively (Figure 2B and C, Supplementary Figure S4), indicating that only

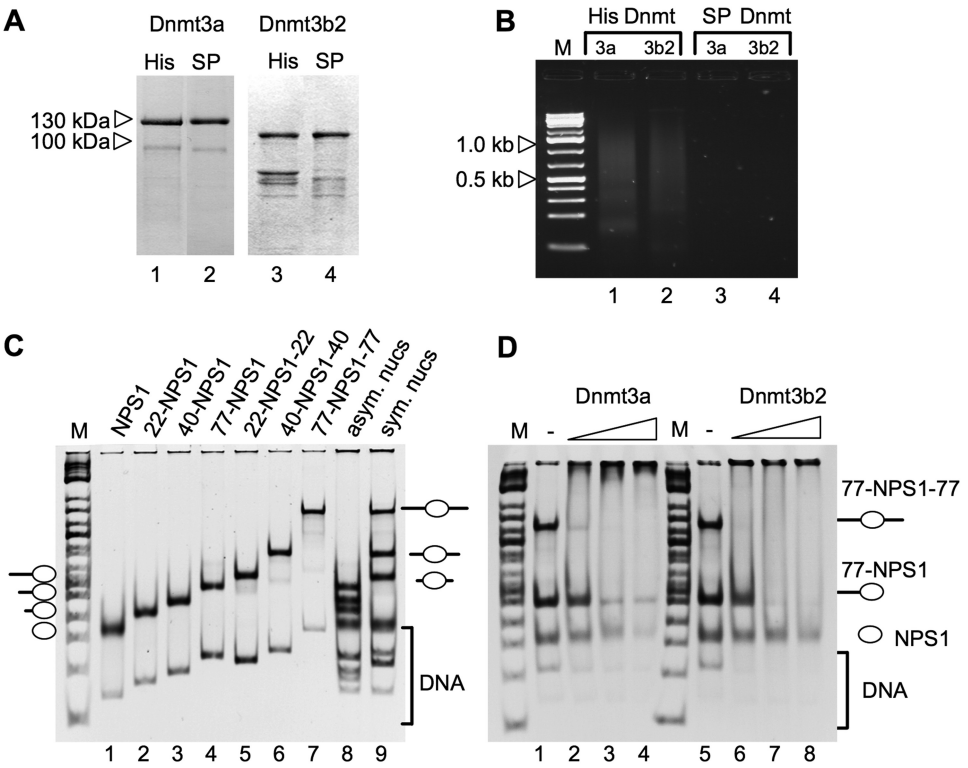

Figure 1. Dnmt3a and Dnmt3b2 have distinct substrate binding properties. (**A**) His-tagged Dnmt3a and Dnmt3b2 were purified using Ni-NTA columns (lanes 1 and 3), followed by cation exchange chromatography (SP-Sepharose; lanes 2 and 4). Proteins were subjected to SDS–PAGE and Coomassie Blue staining. Sizes of the molecular weight marker are indicated. (**B**) Dnmt3a and Dnmt3b2 (His Dnmt; lanes 1 and 2) isolated only by His-tag-affinity purification, or by His-tag- and subsequent cation exchange purification (SP Dnmt; lanes 3 and 4) were analysed for co-purifying DNA contaminations. Five micrograms of each protein preparation was incubated with RNaseA and proteinaseK. The remaining DNA was purified and analysed by agarose gel electrophoresis and staining with ethidium bromide. Molecular weight marker (M) and sizes are indicated. (**C**) DNA fragments containing the NPS1 sequence located either in the centre of the DNA or close to the DNA border were partially assembled into mononucleosomes using the salt dialysis method. The sizes of the linker DNA next to the NPS1 sequences are indicated. (**D**) Different nucleosomal templates were mixed in 1:1 ratio (lanes 1 and 5) and incubated with a 3.5- to 15-fold molar excess of Dnmt3a and Dnmt3b2 (lanes 2–4 and 6–8). Reactions were analysed by native polyacrylamide gel electrophoresis next to a molecular weight marker (M).

every second nucleosome should contain a single methylated CpG dinucleotide within the nucleosomal region. This result clearly shows a strong reduction of DNA methylation towards nucleosomes, and indicates that DNA wrapped around the histone octamer represents a major obstacle to *de novo* DNA methylation *in vitro*.

As we have shown above, Dnmt3a and Dnmt3b2 bind efficiently to symmetric nucleosomes with long DNA linkers. Therefore, we analysed the N78-NPS2-N79 nucleosome, an optimal substrate for both *de novo* methyltransferases, lacking CpG sites in the DNA linker (Figure 2A). Dnmt3a- and Dnmt3b2-mediated nucleosomal DNA methylation was repressed on this template by 6.8- and 4.5-fold, respectively (Figure 2B and C). Repression was significantly lower as for the linker-free NPS2 nucleosome. However, also the M.SssI-dependent repression was reduced to 16.1-fold for this template, showing that the substrate still maintained accessible CpG sites (Figure 2B and C). Compared to M.SssI, the mammalian enzymes exhibited 2- to 4-fold higher nucleosomal methylation activities, suggesting a low level of nucleosomal DNA methylation. However, this assay does not allow to quantify and to identify the sites of nucleosomal DNA methylation.

De novo methylation occurs at the borders of the nucleosomes

To reveal the extent of nucleosomal DNA methylation we conducted a detailed site-specific CpG methylation analysis of free and nucleosomal C91-NPS2-C104 with Dnmt3a, Dnmt3b2 and M.SssI using bisulfite conversion (Figure 3). After stopping the DNA methylation reaction, the purified DNA was treated with bisulfite, resulting in the deamination of the non-methylated cytosine residues to uracil. DNA templates were amplified by PCR, cloned and the DNA methylation pattern was subsequently analysed by sequencing of individual clones. In contrast to the incorporation of ^{3}H- or ^{14}C-labelled methyl-groups, following scintillation counting or PAGE-based quantification, respectively, this technique allows a quantitative and qualitative evaluation of DNA methylation events on the (+) and (−) DNA strand at the same time.

As expected, the bacterial DNA methyltransferase M.SssI efficiently methylated all CpG sites on both the (+) and the (−) strand of the free DNA (Figure 3A, light grey) and only the protein free DNA of the nucleosomal template (Figure 3A, dark grey). Visual inspection and the calculated DNA:NUC methylation ratio of

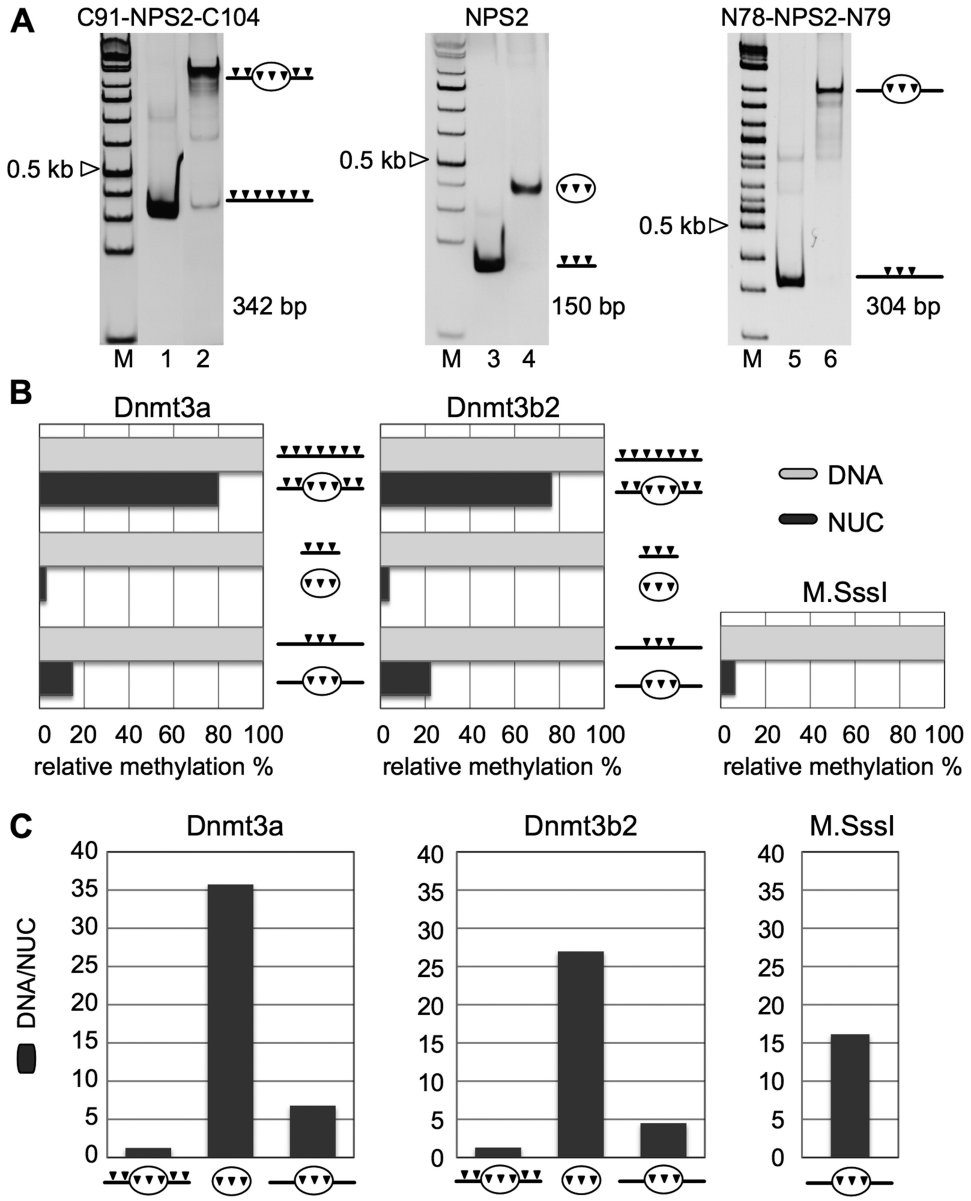

Figure 2. Nucleosomes are major obstacles for *de novo* DNA methylation *in vitro*. (**A**) DNA templates containing the NPS2 sequence either with linker DNA containing CpG sites (C91-NPS2-C104, 12 CpG sites in linker, lanes 1 and 2), without linker DNA (NPS2, 15 CpG sites, lanes 3 and 4) or with linker DNA depleted of CpG sites (N78-NPS2-N79, lanes 5 and 6) were fully reconstituted into mononucleosomes. Nucleosomes were analysed by native PAGE next to a molecular weight marker (M). Black triangles (filled inverted triangle) indicate CpG sites. (**B**) Free DNA and nucleosomes described in (A) were subjected to *in vitro* DNA methylation reactions with the indicated DNA methyltransferases. The incorporation of the ^{3}H-methyl was quantified and the methylation efficiency (given as percentage relative to free DNA) is plotted. Black triangles indicate CpG sites and the oval indicates the position of the nucleosome. (**C**) The ratios of the methylation efficiencies of DNA compared to nucleosomes (DNA/NUC) are given for the indicated nucleosomal templates. Black triangles indicate CpG sites and the oval indicates the position of the nucleosome.

160 clearly shows a perfect nucleosomal substrate, omitting free DNA and having all nucleosomes perfectly positioned on the NPS2 sequence. The overall DNA methylation efficiency of Dnmt3a and Dnm3b2 towards free DNA was reduced compared to M.SssI (Figure 3A), however our enzymes exhibited a 2- to 3-fold higher methylation efficiency compared to enzymes preparations used in previous studies (42). The different *de novo* DNA methylation patterns of Dnmt3a and Dnmt3b2 on free DNA may be contributed to sequence preferences (43) or distributive and processive DNA methylation mechanisms of the enzymes (28) (Figure 3A, light grey).

Visual inspection clearly shows that the accessible linker DNA is efficiently methylated by Dnmt3a and Dnmt3b2 and that the nucleosomal DNA is refractory to DNA methylation. If nucleosomal DNA methylation events are observed, they are located at CpG sites close to the entry/exit sites of the nucleosomes and are not distributed along the entire nucleosome (Figure 3A). Comparing the

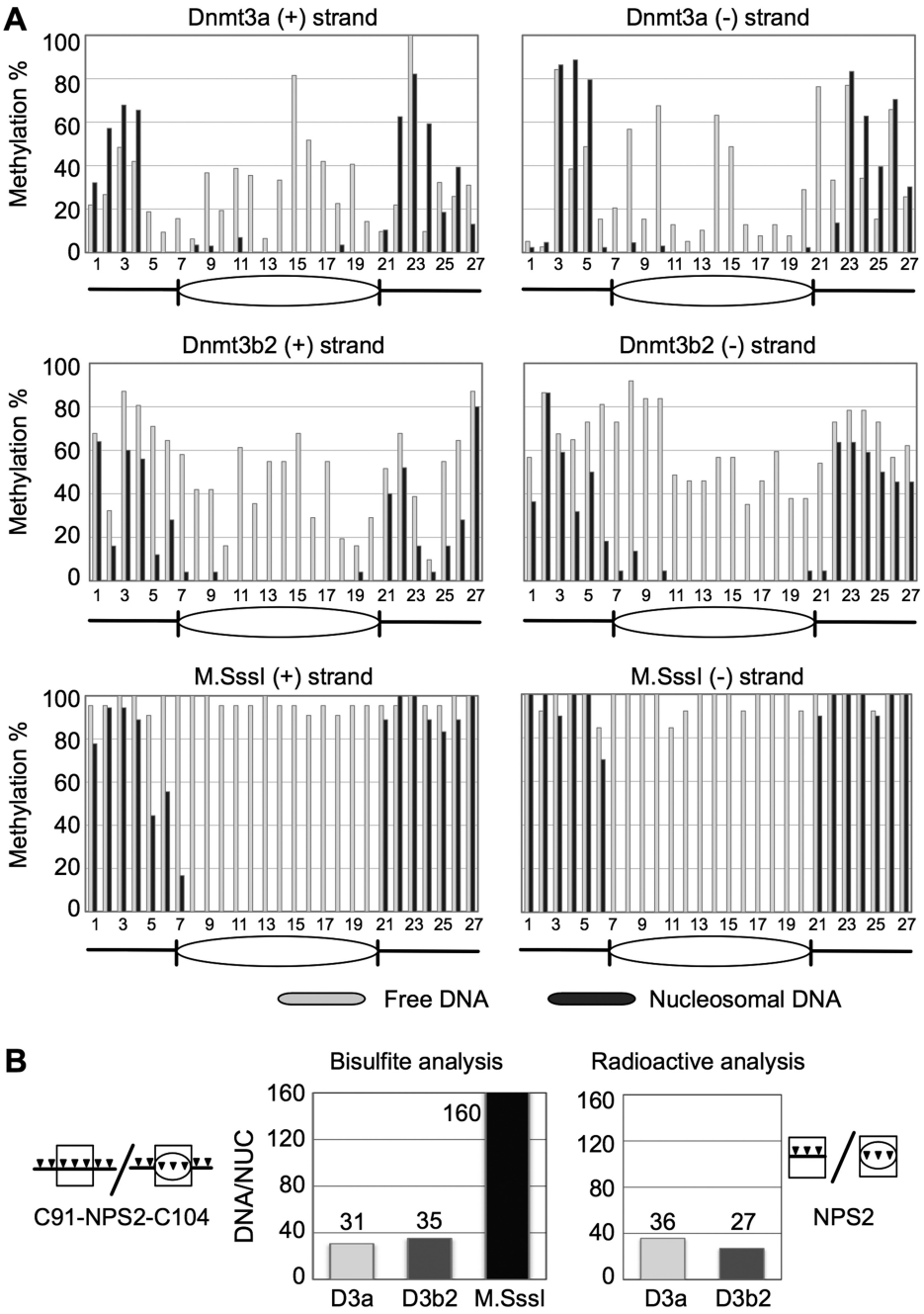

Figure 3. *De novo* DNA methylation is limited to the entry/exit sites of the nucleosome. (**A**) DNA methylation reactions of the *de novo* DNA methyltransferases and M.SssI with the free DNA or the nucleosomal DNA fragment C91-NPS2-C104 were subjected to bisulfite conversion. The methylation frequency for each CpG site is plotted against the CpG sites of the DNA sequence. Analysis of the free DNA (light grey) and the nucleosomal template (dark grey) for the (+) strand and the (−) strand is shown. The position of the nucleosome is indicated. On average 20–40 sequences for each strand were sequenced. (**B**) The ratio of methylation events within the NPS2 sequence (black box, filled inverted triangle arrows indicated CpG sites) of DNA and nucleosomes as an average of the (+) and the (−) strand was calculated for C91-NPS2-C104 from the bisulfite experiments, and for NPS2 from the radioactive assay. The DNA/NUC ratios are indicated in the figure.

M.SssI data with the *de novo* methyltransferases clearly suggest that the latter have a low nucleosomal DNA methylation activity.

The radioactive DNA methylation assay perfectly matches the bisulfite analysis as revealed by the quantitative evaluation of the nucleosomal DNA methylation. Calculations of the DNA:NUC ratios of DNA methylation from the bisulfite-treated sequences and the radioactive assay using the NPS2 DNA fragment give rise to ratios between 27 and 35 (Figure 3B). This corresponds to 2.8–.7% of nucleosomal DNA methylation by the *de novo* methyltransferases. Hence, the observed reduction of nucleosomal DNA methylation (Figure 2B, NPS2) was not due to different Dnmt/nucleosome binding affinities (Figure 1C, Supplementary Figure S2) but due to the inaccessibility of CpG sites.

Remodelled nucleosomes are preferential targets for Dnmt3a

Next we addressed whether ATP-dependent nucleosome remodelling has an effect on DNA methylation. We reconstituted nucleosomes on the N78-NPS2-N79 DNA, placing the nucleosome on the CpG containing center of the DNA fragment (Supplementary Figure S6A). Snf2H repositions this nucleosome in the presence of ATP to a site close to the DNA end, thereby exposing the majority of CpG sites (Figure 4A, Supplementary Figure S6B–D). Nucleosome remodelling in the presence of non-hydrolysable ATPγS and the ATPase mutant Snf2H K211R served as controls (Figure 4A, Supplementary Figure S1).

Nucleosome remodelling reactions were supplemented with either M.SssI or the *de novo* DNA methyltransferases and incubated for 10 and 30 min with ^{3}H-SAM. Radioactive signals were quantified and normalized to the methyltransferase activity on free DNA (Figure 4B). M.SssI was severely inhibited by the nucleosomal template demonstrating the high quality of the positioned nucleosome. However, it has to be mentioned that repression was not as efficient as shown in Figure 2, as the nucleosomal batch contained slightly elevated levels of free DNA. Active remodelling by the addition of Snf2H and ATP results in the efficient relocation of the nucleosome to the border of the DNA fragment (Figure 4A, lane 4). However, only ~50% of the CpG sites were rendered accessible as monitored by M.SssI methylation (Figure 4B, lane 6).

Due to the nucleosomal DNA methylation activity of the *de novo* methyltransferases, nucleosomal methylation was less reduced as compared to M.SssI (Figure 4B). However, active chromatin remodelling resulted in a DNA methylation activity comparable to free DNA in the case of Dnmt3b2 (Figure 4B, lane 12). Nucleosomal methylation activity of Dnmt3a was inhibited like for Dnmt3b2, but the enzymes behaved differently on the remodelled substrate. Unexpectedly, the DNA methylation efficiency of Dnmt3a for the remodelled nucleosome was almost twice as high as for the free DNA (Figure 4B, lane 18), suggesting that Dnmt3a does preferentially recognize the remodelled substrate. The increase in DNA methylation is dependent on the Snf2H dependent remodelling activity, as Snf2H-K211R, the ATPase mutant that cannot move nucleosomes any more, fails to increase the DNA methylation levels.

To test for differences in Dnmt3a binding to the non-remodelled and remodelled substrates we performed

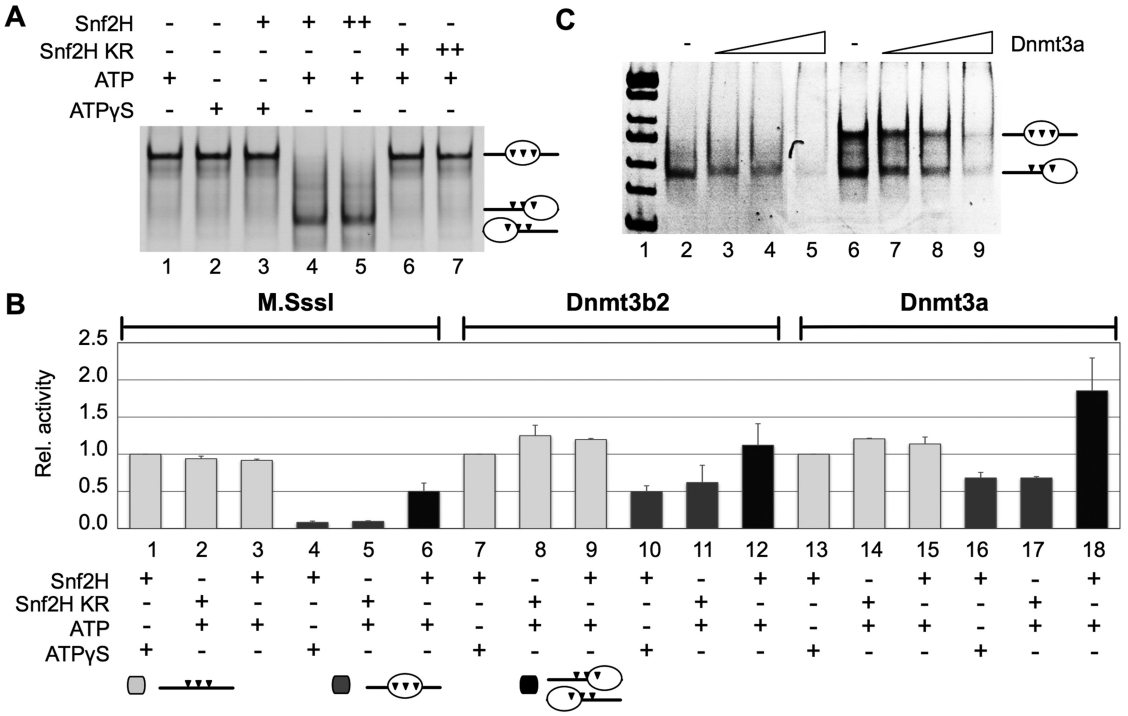

Figure 4. Chromatin remodelling stimulates *de novo* DNA methylation. (**A**) Chromatin remodelling reactions were performed in the presence of WT Snf2H (lanes 3–5) or mutant Snf2H K211R (lanes 6 and 7) using a 0.7–1.5 molar ratio (+, ++) relative to the nucleosomal N78-NPS2-N79 DNA. Reactions were supplied with ATP or ATPγS as indicated and stopped by the addition of competitor DNA. Nucleosome positions were analysed by native PAGE. Arrows (filled inverted triangle) indicate CpG sites on the DNA fragment. Black triangles indicate CpG sites and the oval indicates the position of the nucleosome. (**B**) Remodelling reactions were performed as indicated using either nucleosomal (dark grey bars) or free DNA (light grey bars). DNA methylation with the indicated enzymes was performed for 10 min. The incorporation of ^{3}H-methyl groups was measured and the relative methylation activity (normalized to free DNA) of free DNA and nucleosomes was plotted. Black bars mark the reactions on the remodelled substrates. Black triangles indicate CpG sites and the oval indicates the position of the nucleosome. (**C**) Competitive nucleosome-Dnmt3a EMSA. Either the remodelled nucleosomal template or an equimolar mixture of remodelled and non-remodelled nucleosomes were incubated with a 3.5- to 15-fold molar excess of Dnmt3a (lanes 3–5 and 7–9). Reactions were analysed by native polyacrylamide gel electrophoresis next to a molecular weight marker (lane 1). Black triangles indicate CpG sites and the oval indicates the position of the nucleosome.

competitive electromobility shift experiments. We mixed remodelled and non-remodelled nucleosomes at equimolar ratios and incubated them with increasing amounts of Dnmt3a (Figure 4C, Supplementary Figure S6). In contrast to the preferential binding of symmetric over asymmetric nucleosomes by Dnmt3a (Figure 1D), Dnmt3a did not reveal preferential binding to the symmetric nucleosome over the remodelled nucleosome. The affinity of Dnmt3a was significantly increased to the remodelled nucleosome, suggesting to play a role in increasing the DNA methylation rates. An additional explanation for the higher nucleosomal DNA methylation rates comes from the Peter Jones laboratory, suggesting that Dnmt3a does preferentially bind to nucleosomes containing methylated DNA (44). Dnmt3b was shown to interact with Snf2H *in vivo* (23), however, we can exclude a direct stimulatory effect of the remodeller as competitor DNA disrupted nucleosome-remodeller interactions (Supplementary Figure S6B). In addition, Snf2H was used in a 4-fold lower molar ratio compared to Dnmt3a and Dnmt3b2 and Snf2H binding would have been visible in the competitive EMSAs.

Nucleosomal DNA is devoid of DNA methylation in vivo

Current studies on the sites and levels of cellular DNA methylation make use of the free genomic DNA, ignoring its chromatin organization. We established a protocol to directly quantify the extent of nucleosomal and linker DNA methylation, relative to absolute nucleosome positions *in vivo*. In order to determine the chromatin-dependent levels of DNA methylation, we purified nucleosomal DNA from HeLa cells. HeLa chromatin was partially hydrolysed with MNase and the DNA was purified. The resulting nucleosomal ladder exhibited a defined size distribution of DNA fragments, ranging from mono- to tetranucleosomal sizes (Figure 5A, lane 2). At high MNase concentrations the mononucleosomal DNA corresponds to the core-nucleosomal DNA lacking associated DNA-linkers. Accordingly, the isolated nucleosomal-core DNA corresponds to ~150 bp in length (data not shown). The corresponding mono-, di- and trinucleosomal DNA fragments were purified (Figure 5A, lanes 3–5) and used for the subsequent quantification of DNA methylation levels with an enzyme-linked assay (Figure 5B). Interestingly, as seen for the *in vitro* DNA methylation assays (Figures 2 and 3) we see a low level of DNA methylation of the nucleosomal DNA (mononucleosomes) that increases only slightly with increasing DNA concentration (25–200 ng). In contrast, trinucleosomal DNA, harbouring two accessible linker regions, exhibits much stronger DNA methylation levels. This stunning result suggests that DNA methylation is rather depleted within the nucleosomal DNA and exists preferentially in the linker region in between the nucleosomes. Our data suggest that on a global scale nucleosomes are major obstacles for DNA methylation *in vivo*. Comparison of 1 n, 2 n, 3 n nucleosomal DNA revealed a gradual increase in CpG methylation with nucleosomal repeat length, reflecting the relative fraction of DNA linkers present in the substrate (Figure 5B). To exclude possible effects of DNA length on the assay readout and to prove quantification, we generated a methylated and a non-methylated control DNA of 150 bp length (NPS2; Supplementary Figure S5A), showing robust quantification of the data by the enzyme-linked assay (Figure 5B).

Reduced nucleosomal DNA methylation levels were also not a result of reduced CpG levels in the nucleosomal core, as revealed by a re-methylation assay. We compared the *in vitro* methylation activity of M.SssI on sonified genomic DNA of nucleosomal size and the purified mononucleosomal DNA (Supplementary Figure S5B). The result clearly shows a similar number of potential methylatable sites, arguing against the absence of CpG dinucleotides within nucleosomes.

To verify the results obtained with the ELISA assay we quantified nucleosomal and DNA linker methylation with an independent method. Mononucleosomal and genomic DNA 5-methyl cytosine (5-meC) content was quantified using micellar capillary electrophoresis (Figure 5C) according to established protocols (37). With this method molecules are separated on the basis of differences in size, charge, structure and hydrophobicity at high voltages. Gel purified genomic DNA and mononucleosomal DNA were hydrolysed to nucleosides using P1 nuclease and antarctic phosphatase and separated by micellar capillary electrophoresis. The area values of 5-meC and Cytosine were calculated with the carat-software of the Beckman capillary electrophoresis system.

As a result of 10 independent runs, using different DNA batches, mononucleosomal DNA and total genomic DNA exhibited 1.95% ($\pm$0.12%) and 3.06% ($\pm$0.7%) of 5-meC levels, respectively. The reduced DNA methylation levels of nucleosomal DNA are highly significant as revealed by a paired *t*-test (3.1^{-12}) and confirm the results of the ELISA assay. The measured levels of 5-meC in HeLa genomic DNA corresponds very well to the literature values (37), confirming the quantitative robustness of this method. The obtained values allow us to estimate global DNA methylation levels in nucleosomal versus linker DNA. The relative 5-meC content of linker and nucleosomal DNA was determined considering an average nucleosomal repeat length of 188 bp in HeLa cells (38) and a nucleosomal DNA length of 147 bp. We also considered an equal distribution of CpG dinucleotides along the DNA, neglecting the 6.8% CpG sites within CpG islands (45). The total of methylated CpG sites was calculated as the percentage of the proportion of linker DNA added to the proportion of nucleosomal DNA multiplied with the relative nucleosomal 5-meC content. According to these assumptions we calculated a 2-fold higher methylation level of the linker DNA compared to the nucleosomal DNA (Figure 5D).

DISCUSSION

In this study we examined the binding characteristics of Dnmt3a and Dnmt3b2 towards mononucleosomes exhibiting DNA linkers of varying length, the *de novo* DNA methylation of nucleosomes *in vitro* and the effect

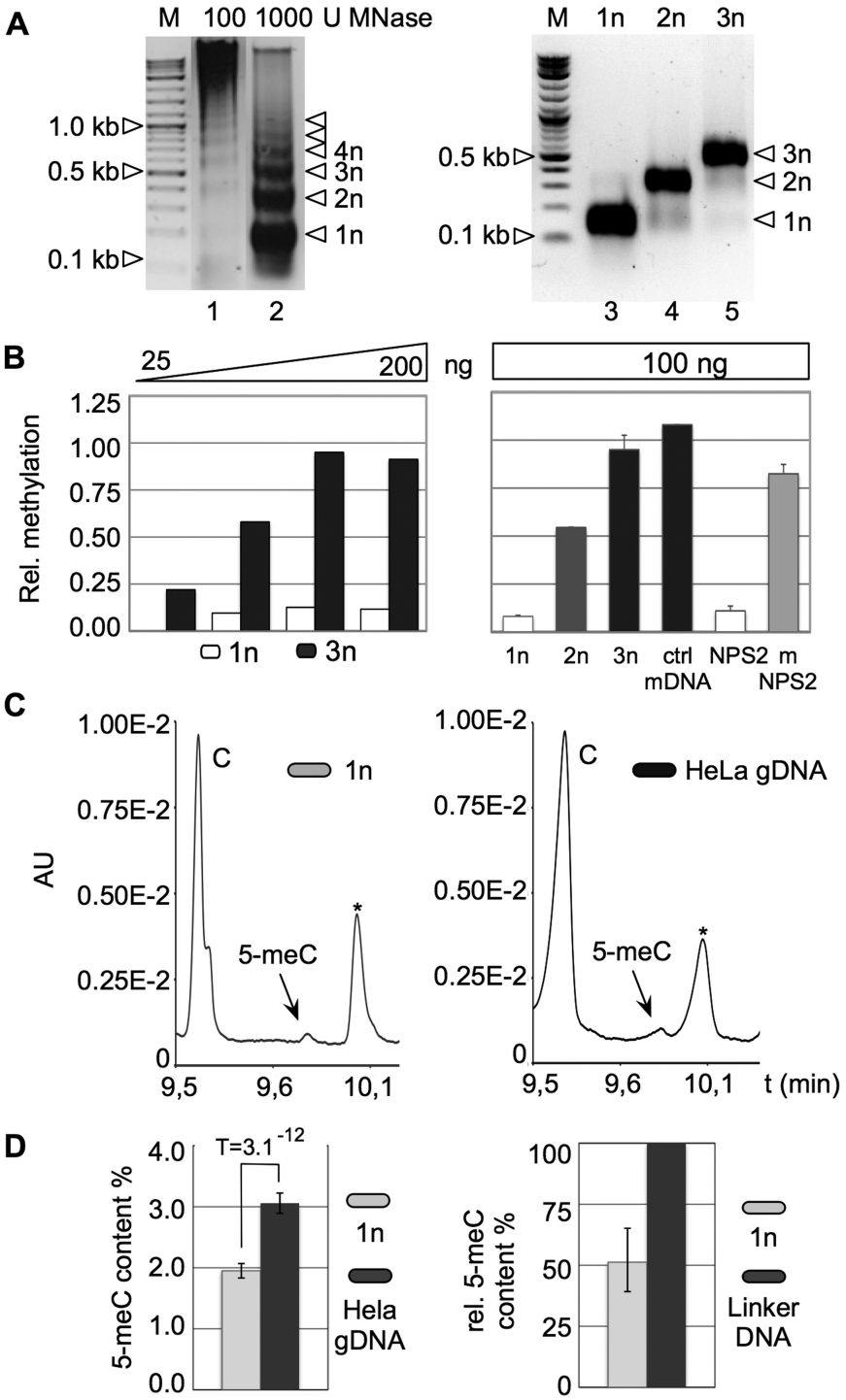

Figure 5. Nucleosomal DNA is devoid of CpG methylation *in vivo*. (**A**) Chromatin from HeLa cells was partially hydrolysed with MNase (lanes 1 and 2) and the purified DNA was analysed by agarose gel electrophoresis. The nucleosome-sized DNA fragments are indicated on the right. Mono-, di- and tri-nucleosomal (1 n, 2 n, 3 n) DNA was isolated and analysed (lanes 3–5). Molecular weight marker (M) and DNA sizes are indicated. (**B**) DNA methylation levels for mononucleosomal (white bars) and trinucleosomal (black bars) DNA using increasing DNA amounts, was determined with a meCpG-sensitive ELISA assay (Sigma). A comparative DNA methylation analysis for 100 ng of different nucleosomal DNAs (1 n, 2 n, 3 n), methylated control DNA (ctrl mDNA), non-methylated and methylated NPS2 DNA (mNPS2) is shown. (**C**) Micellar capillary electrophoresis of nucleosides (~4 μg/μl) from purified and hydrolysed mononucleosomal DNA (left) and genomic HeLa DNA (right). The absorbance (AU) is plotted against the migration time (t; min). The peaks for 2′-deoxycytidine (C), 5-methyl 2′-deoxycytidine (5-meC) and an impurity (asteriks) are indicated. (**D**) The average ($n = 10$) of the 5-meC content of mononucleosomal (light grey) and Hela genomic DNA (dark grey) was calculated as percentage of (Area 5-meC/(Area C + Area 5-meC). Statistical significance of the data was calculated using the paired *t*-test. The calculated 5-meC content of mononucleosomal DNA (light grey, 147 bp) relative to the 5-meC content of linker DNA (dark grey, 41 bp) is given in the graph on the right.

of Snf2H-dependent nucleosome repositioning on *de novo* DNA methylation. As an advancement to previous studies and important for our detailed analysis, we established protocols to purify highly active recombinant Dnmt3a and Dnmt3b2 free of endogenous DNA (Figure 1A) and prepared high-quality mononucleosomes using the salt dialysis method (Figure 2A, Supplementary Figures S3A and S6A). The bacterial CpG-specific DNA methyltransferase M.SssI served as a crucial internal control that allowed us to assess positioning of our nucleosomes and the level of contaminating free DNA in the reaction. Essentially, M.SssI-dependent DNA methylation is inhibited by the DNA bound histone octamer (41).

In agreement with previous findings, EMSAs (Figure 1D, Supplementary Figure S2A and B) revealed that Dnmt3a bound to free DNA and nucleosomes with short linker DNA with similar affinity (21,32). However, we clearly demonstrate preferential binding of Dnmt3a to the mononucleosome 77-NPS1-77, showing that Dnmt3a is able to recognize specific nucleosomal structures. In contrast, Dnmt3b2 showed similar affinities towards DNA and mononucleosomes with long linker DNA (i.e. 77-NPS1-77). The DNA is the preferred substrate, as symmetric and asymmetric nucleosomes and nucleosomes without DNA overhangs are bound in a hierarchic order (Figure 1D, Supplementary Figure S2A and B). Recently, the ADD-domains of Dnmt3a and Dnmt3b were shown to bind similar well to the non-modified histone H3 tail (42), however, we show that the DNA linkers present a much better substrate for the enzymes (Figure 1D, Supplementary Figure S2A–C). The importance of linker DNA binding was also shown by Takeshima and co-workers, showing the modulation of Dnmt3a binding to the DNA linkers by histone H1 (33). Different binding characteristics of Dnmt3a and Dnmt3b2 towards DNA and nucleosomes are probably reflected by differences in the DNA interacting domains. Next to the catalytic domain, the PWWP-domain was shown to bind to DNA. The PWWP-domain of Dnmt3b showed higher DNA binding affinities than Dnmt3a (46), consistent with a lower K_M-value of Dnmt3b for free DNA (26). These results do support our findings in that DNA is the preferred substrate for Dnmt3b2. However, besides the characterized PWWP-domain other regions of the proteins may be involved in the modulation of the nucleosomal binding properties.

With our elaborate *in vitro* analysis of nucleosomal DNA methylation by means of incorporation of ^{3}H-methyl groups into the DNA (Figure 2B and C) or bisulfite treatment of methylated DNA (Figure 3), we are now able to reveal a precise picture of *de novo* DNA methylation in chromatin. Free DNA overhangs were preferentially methylated (Figure 3A), whereas DNA methylation of Dnmt3a and Dnmt3b2 within the region of the nucleosome was strongly reduced to 2.8–3.7% of the CpG levels (Figure 3A and B). An inhibitory effect of the nucleosomal structure on DNA methylation has been shown for Dnmt3a and Dnmt3b2 (21,32,33), however, our results show a much higher protection by the nucleosome as previously reported. Experiments showing similar Dnmt3a-dependent methylation efficiency of free DNA and mononucleosomes are probably the result of DNA contaminations within the enzyme preparations (30). In contrast to our results, Takeshima and colleagues observed significant nucleosomal DNA methylation with Dnmt3b and M.SssI (32). Considering the enzymatic properties of M.SssI (41) and the high affinity of Dnmt3b for naked DNA (26) it is rather tempting to speculate that nucleosomal preparations were not fully reconstituted and still contained free DNA in the reaction.

A recent study applying similar approaches showed efficient *de novo* methylation of DNA linkers and reduced levels of nucleosomal DNA methylation spreading throughout the nucleosome (42). As the authors did not include a M.SssI control it could be that low levels of free DNA were present in the reaction. Most strikingly, our analysis demonstrates that the low-level nucleosomal DNA methylation of Dnmt3a and Dnmt3b2 was limited to the entry/exit sites of the nucleosome and did not spread along the entire nucleosomal region.

The functional correlation of ATP-dependent chromatin remodelling enzymes and DNA methylation *in vivo* has been described (47). In particular, Lsh, a member of the SNF2 superfamily of helicases, was shown to be essential for genome-wide DNA methylation (14) and to influence *de novo* DNA methylation levels (15), through recruitment of Dnmt3b (16,17,48). Similarly, we observe that chromatin remodelling activity is required to generate DNA access and to allow nucleosomal DNA methylation (Figure 4). However, the Dnmt3a DNA methylation efficiency was increased almost 2-fold on the repositioned nucleosome, resulting in a DNA methylation efficiency superior to free DNA. This result suggests that the remodelled nucleosome presents a specialized substrate, stimulating the activity of Dnmt3a.

Indeed, we were able to show that Dnmt3a exhibits a relatively higher affinity to the remodelled nucleosome as to asymmetric positioned nucleosomes. The higher affinity towards the remodelled nucleosome and the fact that Dnmt3a binds with higher affinity to methylated nucleosomal DNA may explain the elevated DNA methylation levels in remodelled nucleosomes (44). Augmented DNA methylation may be in part a result of a particular chromatin structure established by the remodelling enzyme, which is recognized as a preferential substrate by the DNA methyltransferases. With respect to the data of the Jones laboratory, we suggest that the initial methylation of the remodelled nucleosome converts it into a high affinity substrate that is even methylated better than free DNA. Differential substrate binding features and the higher activity of Dnmt3a for remodelled nucleosomes may hint to functional differences and distinct localizations of the methyl transferases, depending on the chromatin structure in the cell. Future experiments will address the mechanism of efficient nucleosomal DNA methylation in kinetically resolved assay systems.

For the first time, we directly quantified the levels of nucleosomal DNA methylation *in vivo*. By the isolation of nucleosomal core fragments, we were able to quantify the different levels of DNA methylation between

nucleosomal and genomic DNA. Whereas the enzyme-linked assay indicated strong differences in DNA methylation levels, only the micellar capillary electrophoresis system was suitable to provide a quantitative measure. The global maintenance of a 2-fold difference in nucleosomal versus linker DNA methylation levels gives important insights into the dynamics of chromatin structure *in vivo* and the mechanisms of DNA methylation. As we have shown, the nucleosome is refractory to DNA methylation, and ATP-dependent chromatin dynamics is required to circumvent nucleosomal inaccessibility. Low levels of nucleosomal DNA methylation *in vivo* suggest a rather non-dynamic chromatin structure in the cell, with nucleosomes occupying the same sites throughout the cell cycle. Indicating that the activity of the numerous chromatin remodelling machines is highly restricted and maintain specific chromatin structures (12,49), rather than creating fluid chromatin structures that are accessible to any kind of DNA modification. Our analysis gives insights on the distribution of DNA methylation on a global scale. We suggest that local DNA methylation patterns, especially at regulatory regions, may escape this rule of nucleosomal depletion, as active chromatin remodelling occurs at these sites.

The nucleosome position-dependent distribution of DNA methylation could not be detected by the methylome mapping studies, as global nucleosome positioning varies from cell to cell (50). Nucleosome spacing is comparable from cell to cell, but the actual positions are not the same relative to the underlying DNA. High-throughput sequencing approaches to evaluate the DNA methylome, have only generated short sequence reads, that do not resolve nucleosome positioning features (51,52). These assays were not designed to observe the chromatin structure dependent DNA methylation patterns. High-resolution, chromatin-dependent DNA methylation maps will be required to dissect the global and local effects of chromatin structure on the epigenome. In contrast to a recent study showing a very modest increase of 1.2% (from 75% to 76.2%) of nucleosomal DNA methylation compared to the linker DNA (53), we observed a 2-fold decrease of DNA methylation levels within the nucleosome core particles. The discrepancy arises from the used methodology. Whereas we did directly quantify DNA methylation levels, Pellegrini and coworkers performed a correlation analysis between nucleosome positions and known DNA methylation maps (53). Their analysis ignores the fact that most nucleosome positions vary from cell to cell and that DNA methylation maps represent a summary of DNA methylation sites of multiple cells.

In summary, we show that chromatin structure does influence *de novo* DNA methylation *in vitro* and *in vivo*, targeting global DNA methylation to the linker regions of the nucleosomes. This indicates that besides the high levels of remodelling enzymes in the cell, the global chromatin structure *in vivo* is not fluid. We hypothesize that DNA methylation is only actively changed at regulatory sites where differential recruitment of remodelling enzymes actively changes the chromatin structure and DNA accessibility.

SUPPLEMENTARY DATA

Supplementary Data are available at NAR Online.

FUNDING

The Deutsche Forschungsgemeinschaft (DFG); Bayerisches Genomforschungsnetzwerk (BayGene); by BMBF, partners of the ERASysBio+ (to G.L.). Funding for open access charge: DFG.

Conflict of interest statement. None declared.

REFERENCES

1. Jones,P.A. and Baylin,S.B. (2002) The fundamental role of epigenetic events in cancer. *Nat. Rev. Genet.*, **3**, 415–428.
2. Bird,A. (2002) DNA methylation patterns and epigenetic memory. *Genes Dev.*, **16**, 6–21.
3. Li,E. (2002) Chromatin modification and epigenetic reprogramming in mammalian development. *Nat. Rev. Genet.*, **3**, 662–673.
4. Klose,R.J. and Bird,A.P. (2006) Genomic DNA methylation: the mark and its mediators. *Trends Biochem. Sci.*, **31**, 89–97.
5. Freitag,M. and Selker,E.U. (2005) Controlling DNA methylation: many roads to one modification. *Curr. Opin. Genet. Dev.*, **15**, 191–199.
6. Hermann,A., Gowher,H. and Jeltsch,A. (2004) Biochemistry and biology of mammalian DNA methyltransferases. *Cell. Mol. Life Sci.*, **61**, 2571–2587.
7. Längst,G. and Becker,P.B. (2004) Nucleosome remodeling: one mechanism, many phenomena? *Biochim. Biophys. Acta*, **1677**, 58–63.
8. Felsenfeld,G. and Groudine,M. (2003) Controlling the double helix. *Nature*, **421**, 448–453.
9. Khorasanizadeh,S. (2004) The nucleosome: from genomic organization to genomic regulation. *Cell*, **116**, 259–272.
10. Flaus,A., Martin,D.M.A., Barton,G.J. and Owen-Hughes,T. (2006) Identification of multiple distinct Snf2 subfamilies with conserved structural motifs. *Nucleic Acids Res.*, **34**, 2887–2905.
11. Clapier,C. and Cairns,B. (2009) The Biology of Chromatin Remodeling Complexes. *Annu. Rev. Biochem.*, **78**, 273–304.
12. Rippe,K., Schrader,A., Riede,P., Strohner,R., Lehmann,E. and Längst,G. (2007) DNA sequence- and conformation-directed positioning of nucleosomes by chromatin-remodeling complexes. *Proc. Natl Acad. Sci. USA*, **104**, 15635–15640.
13. Bartee,L. and Bender,J. (2001) Two Arabidopsis methylation-deficiency mutations confer only partial effects on a methylated endogenous gene family. *Nucleic Acids Res.*, **29**, 2127–2134.
14. Dennis,K., Fan,T., Geiman,T., Yan,Q. and Muegge,K. (2001) Lsh, a member of the SNF2 family, is required for genome-wide methylation. *Genes Dev.*, **15**, 2940–2944.
15. Zhu,H., Geiman,T.M., Xi,S., Jiang,Q., Schmidtmann,A., Chen,T., Li,E. and Muegge,K. (2006) Lsh is involved in de novo methylation of DNA. *EMBO J.*, **25**, 335–345.
16. Xi,S., Zhu,H., Xu,H., Schmidtmann,A., Geiman,T.M. and Muegge,K. (2007) Lsh controls Hox gene silencing during development. *Proc. Natl Acad. Sci. USA*, **104**, 14366–14371.
17. Myant,K. and Stancheva,I. (2008) LSH cooperates with DNA methyltransferases to repress transcription. *Mol. Cell. Biol.*, **28**, 215–226.
18. Gibbons,R.J., McDowell,T.L., Raman,S., O'Rourke,D.M., Garrick,D., Ayyub,H. and Higgs,D.R. (2000) Mutations in ATRX, encoding a SWI/SNF-like protein, cause diverse changes in the pattern of DNA methylation. *Nat. Genet.*, **24**, 368–371.
19. Strohner,R., Nemeth,A., Jansa,P., Hofmann-Rohrer,U., Santoro,R., Längst,G. and Grummt,I. (2001) NoRC–a novel member of mammalian ISWI-containing chromatin remodeling machines. *EMBO J.*, **20**, 4892–4900.

20. Santoro,R. and Grummt,I. (2005) Epigenetic mechanism of rRNA gene silencing: temporal order of NoRC-mediated histone modification, chromatin remodeling, and DNA methylation. *Mol. Cell. Biol.*, **25**, 2539–2546.
21. Robertson,A.K., Geiman,T.M., Sankpal,U.T., Hager,G.L. and Robertson,K.D. (2004) Effects of chromatin structure on the enzymatic and DNA binding functions of DNA methyltransferases DNMT1 and Dnmt3a in vitro. *Biochem. Biophys. Res. Commun.*, **322**, 110–118.
22. Datta,J., Majumder,S., Bai,S., Ghoshal,K., Kutay,H., Smith,D.S., Crabb,J.W. and Jacob,S.T. (2005) Physical and functional interaction of DNA methyltransferase 3A with Mbd3 and Brg1 in mouse lymphosarcoma cells. *Cancer Res.*, **65**, 10891–10900.
23. Geiman,T.M., Sankpal,U.T., Robertson,A.K., Zhao,Y., Zhao,Y. and Robertson,K.D. (2004) DNMT3B interacts with hSNF2H chromatin remodeling enzyme, HDACs 1 and 2, and components of the histone methylation system. *Biochem. Biophys. Res. Commun.*, **318**, 544–555.
24. Pradhan,S., Bacolla,A., Wells,R.D. and Roberts,R.J. (1999) Recombinant human DNA (cytosine-5) methyltransferase. I. Expression, purification, and comparison of de novo and maintenance methylation. *J. Biol. Chem.*, **274**, 33002–33010.
25. Aoki,A., Suetake,I., Miyagawa,J., Fujio,T., Chijiwa,T., Sasaki,H. and Tajima,S. (2001) Enzymatic properties of de novo-type mouse DNA (cytosine-5) methyltransferases. *Nucleic Acids Res.*, **29**, 3506–3512.
26. Suetake,I., Miyazaki,J., Murakami,C., Takeshima,H. and Tajima,S. (2003) Distinct enzymatic properties of recombinant mouse DNA methyltransferases Dnmt3a and Dnmt3b. *J. Biochem.*, **133**, 737–744.
27. Gowher,H. and Jeltsch,A. (2001) Enzymatic properties of recombinant Dnmt3a DNA methyltransferase from mouse: the enzyme modifies DNA in a non-processive manner and also methylates non-CpG [correction of non-CpA] sites. *J. Mol. Biol.*, **309**, 1201–1208.
28. Gowher,H. and Jeltsch,A. (2002) Molecular enzymology of the catalytic domains of the Dnmt3a and Dnmt3b DNA methyltransferases. *J. Biol. Chem.*, **277**, 20409–20414.
29. Yokochi,T. and Robertson,K.D. (2002) Preferential methylation of unmethylated DNA by Mammalian de novo DNA methyltransferase Dnmt3a. *J. Biol. Chem.*, **277**, 11735–11745.
30. Gowher,H., Stockdale,C.J., Goyal,R., Ferreira,H., Owen-Hughes,T. and Jeltsch,A. (2005) De novo methylation of nucleosomal DNA by the mammalian Dnmt1 and Dnmt3A DNA methyltransferases. *Biochemistry*, **44**, 9899–9904.
31. Okuwaki,M. and Verreault,A. (2004) Maintenance DNA methylation of nucleosome core particles. *J. Biol. Chem.*, **279**, 2904–2912.
32. Takeshima,H., Suetake,I., Shimahara,H., Ura,K., Tate,S.-I. and Tajima,S. (2006) Distinct DNA methylation activity of Dnmt3a and Dnmt3b towards naked and nucleosomal DNA. *J. Biochem.*, **139**, 503–515.
33. Takeshima,H., Suetake,I. and Tajima,S. (2008) Mouse Dnmt3a Preferentially Methylates Linker DNA and Is Inhibited by Histone H1. *J. Mol. Biol.*, **383**, 810–821.
34. Hakimi,M.-A., Bochar,D.A., Schmiesing,J.A., Dong,Y., Barak,O.G., Speicher,D.W., Yokomori,K. and Shiekhattar,R. (2002) A chromatin remodelling complex that loads cohesin onto human chromosomes. *Nature*, **418**, 994–998.
35. Aalfs,J.D., Narlikar,G.J. and Kingston,R.E. (2001) Functional differences between the human ATP-dependent nucleosome remodeling proteins BRG1 and SNF2H. *J. Biol. Chem.*, **276**, 34270–34278.
36. Längst,G., Bonte,E., Corona,D.F. and Becker,P.B. (1999) Nucleosome movement by CHRAC and ISWI without disruption or trans-displacement of the histone octamer. *Cell*, **97**, 843–852.
37. Fraga,M.F., Uriol,E., Borja Diego,L., Berdasco,M., Esteller,M., Cañal,M.J. and Rodríguez,R. (2002) High-performance capillary electrophoretic method for the quantification of 5-methyl 2′-deoxycytidine in genomic DNA: application to plant, animal and human cancer tissues. *Electrophoresis*, **23**, 1677–1681.
38. Compton,J.L., Bellard,M. and Chambon,P. (1976) Biochemical evidence of variability in the DNA repeat length in the chromatin of higher eukaryotes. *Proc. Natl Acad. Sci. USA*, **73**, 4382–4386.
39. Bock,C., Reither,S., Mikeska,T., Paulsen,M., Walter,J. and Lengauer,T. (2005) BiQ Analyzer: visualization and quality control for DNA methylation data from bisulfite sequencing. *Bioinformatics*, **21**, 4067–4068.
40. Thåström,A., Thåström,A.E.A., Lowary,P.T., Widlund,H.R., Cao,H., Kubista,M. and Widom,J. (1999) Sequence motifs and free energies of selected natural and non-natural nucleosome positioning DNA sequences. *J. Mol. Biol.*, **288**, 213–229.
41. Kladde,M.P., Xu,M. and Simpson,R.T. (1999) DNA methyltransferases as probes of chromatin structure in vivo. *Meth. Enzymol.*, **304**, 431–447.
42. Zhang,Y., Jurkowska,R., Soeroes,S., Rajavelu,A., Dhayalan,A., Bock,I., Rathert,P., Brandt,O., Reinhardt,R., Fischle,W. *et al.* (2010) Chromatin methylation activity of Dnmt3a and Dnmt3a/3L is guided by interaction of the ADD domain with the histone H3 tail. *Nucleic Acids Res.*, **38**, 4246–4253.
43. Handa,V. and Jeltsch,A. (2005) Profound flanking sequence preference of Dnmt3a and Dnmt3b mammalian DNA methyltransferases shape the human epigenome. *J. Mol. Biol.*, **348**, 1103–1112.
44. Sharma,S., De Carvalho,D.D., Jeong,S., Jones,P.A. and Liang,G. (2011) Nucleosomes containing methylated DNA stabilize DNA methyltransferases 3A/3B and ensure faithful epigenetic inheritance. *PLoS Genet.*, **7**, e1001286.
45. Rollins,R.A., Haghighi,F., Edwards,J.R., Das,R., Zhang,M.Q., Ju,J. and Bestor,T.H. (2006) Large-scale structure of genomic methylation patterns. *Genome Res.*, **16**, 157–163.
46. Chen,T., Tsujimoto,N. and Li,E. (2004) The PWWP domain of Dnmt3a and Dnmt3b is required for directing DNA methylation to the major satellite repeats at pericentric heterochromatin. *Mol. Cell. Biol.*, **24**, 9048–9058.
47. Robertson,K.D. (2002) DNA methylation and chromatin - unraveling the tangled web. *Oncogene*, **21**, 5361–5379.
48. Xi,S., Geiman,T.M., Briones,V., Guang Tao,Y., Xu,H. and Muegge,K. (2009) Lsh participates in DNA methylation and silencing of stem cell genes. *Stem Cells*, **27**, 2691–2702.
49. Pham,C.D., He,X. and Schnitzler,G.R. (2010) Divergent human remodeling complexes remove nucleosomes from strong positioning sequences. *Nucleic Acids Res.*, **38**, 400–413.
50. Radman-Livaja,M. and Rando,O.J. (2010) Nucleosome positioning: how is it established, and why does it matter? *Dev. Biol.*, **339**, 258–266.
51. Meissner,A., Mikkelsen,T.S., Gu,H., Wernig,M., Hanna,J., Sivachenko,A., Zhang,X., Bernstein,B.E., Nusbaum,C., Jaffe,D.B. *et al.* (2008) Genome-scale DNA methylation maps of pluripotent and differentiated cells. *Nature*, **454**, 766–770.
52. Lister,R., Pelizzola,M., Dowen,R.H., Hawkins,R.D., Hon,G., Tonti-Filippini,J., Nery,J.R., Lee,L., Ye,Z., Ngo,Q.-M. *et al.* (2009) Human DNA methylomes at base resolution show widespread epigenomic differences. *Nature*, **462**, 315–322.
53. Chodavarapu,R.K., Feng,S., Bernatavichute,Y.V., Chen,P.-Y., Stroud,H., Yu,Y., Hetzel,J.A., Kuo,F., Kim,J., Cokus,S.J. *et al.* (2010) Relationship between nucleosome positioning and DNA methylation. *Nature*, **466**, 388–392.